

Received May 25, 2018, accepted June 18, 2018, date of publication June 27, 2018, date of current version July 25, 2018.

Digital Object Identifier 10.1109/ACCESS.2018.2851018

A Load Identification Algorithm of Frequency Domain Filtering Under Current Underdetermined Separation

XIN WU^{ID}, (Member, IEEE), XIAO HAN, LIYA LIU^{ID}, AND BING QI

³School of Electrical and Electronic Engineering, North China Electric Power University, Beijing 102206, China

Corresponding author: Xin Wu (19861002wuxin@163.com)

This work was supported in part by Natural Science Foundation of Beijing Municipality under Grant 3172034 and in part by the Fundamental Research Funds for the Central Universities of China under Grant 2018MS001.

ABSTRACT Non-intrusive load identification is important to load monitoring and smart power utilization. In order to effectively identify load status and obtain detailed power data, this paper explained a load identification algorithm based on load decomposition and frequency domain filtering. It realized load decomposition through solving an underdetermined problem of a single current signal under non-intrusive collection mode and then further achieved load identification. The underdetermined problem was optimized into a 1-D underdetermined problem. The solving model was constructed as separating the collecting current into two channels. According to the sparseness of the current frequency domain signal, the optimal solution was obtained by a two-step iterative shrinkage threshold algorithm. Therefore, each operation load can be decomposed independently. The frequency-domain filter group was conducted to filter the decomposition current, and load identification was realized based on the decision of the frequency component after filtering. The algorithm simplified the identification complexity, with a fast convergence rate and high identification accuracy. The performance was validated by the actually measured data. The load decomposition and identification was effective, which could accurately determine the load status, and obtain the current waveform of the independent load.

INDEX TERMS Frequency-domain filtering, load decomposition, load identification, non-intrusive load monitoring, solving underdetermined problem.

I. INTRODUCTION

As smart grid develops to move traditional power industry towards highly intensive, knowledge-based and technology-based directions, apart from the quantity and quality of the power generation side, great attention should also be paid to the management of the demand side. Therefore, there is increasing need for intelligence on the power distribution and consumption side [1], [2]. Demand side management (DSM) has been applied to optimize the low voltage user clients for effective load management. The intelligent technologies for power consumption side have aroused more and more interest [3], [4]. The key to DSM is the acquisition of the detailed information about household energy efficiency, analysis of household electric energy consumption structure, and better understanding of the impact of user behaviors on their household energy efficiency, all of which would guide users to consciously take action to conserve energy [5]–[7].

Load monitoring is the core technology for load management. The traditional approach to load monitoring is intrusive, and each power consumption appliance comes with an information acquisition device. Besides, the power supply is interrupted temporarily during their installation and maintenance, which causes inconveniences for users. Therefore, this approach features poor practicality and availability. Because of the above deficiency of intrusive approach, a non-intrusive load monitoring (NILM) approach was proposed by Professor Hart in the 1980s. Instead of intruding the loads, the approach acquires the relevant data at power entrance. It carries out load decomposition and identification based on signal analysis and processing, thus allowing for status identification of all loads on power consumption network [8], [9].

Based on the existing researches, the non-intrusive load identification algorithm is mainly divided into two categories.

One is to switch the judgment based on the changes in load signature; the other is the intelligent identification algorithm based on pattern classification. Load signature refers to those load features which can reliably mark the electricity status of the load [9], [10]. Hart [10] proposed a clustering algorithm based on active and reactive (P-Q) features. Due to the simplicity of this method, it is widely used in NILM research, but this algorithm cannot recognize devices with overlapping P-Q features. Dinesh *et al.* [11], [12] used the uncorrelated component (i.e. frequency component) of the power spectrum of the load signal as an effective feature and relied on the improved mean shift clustering algorithm and Bayesian classification method to estimate the active power of each individual device from the aggregated signal, which can solve the problem raised in [10], but the number of clusters in the recognition process was not prior information, which has an impact on the recognition accuracy. In [13], the entire operation cycle of the load is modeled and the event windows are identified based on load characteristics. The recognition accuracy reaches more than 90%. However, it only identifies the electrical appliances the user is willing to register, and the edges of the unregistered electrical appliances are excluded from the candidate electrical windows. The innovation of [14] is that it develops a new load disaggregation approach to estimate different customer energy consumption at the bulk supply point based on general substation measurement without relying on smart meter data, customer surveys and so on. But the disadvantage of this approach is that it is necessary to conduct off line training for all possible combinations of different loads, which is not conducive to the wide application. In addition, the work in [15] and [16] used the V-I trajectory to identify the load operation. The V-I trajectory of different loads is different, but how to extract the load V-I trajectory from the total system power data in the actual application was not explained in any literature. The main limitation with the steady-state based methods is that they could not accurately identify the multi-state loads and feature overlap phenomena [17]. In order to overcome the limitations of the steady-state analysis methods, [8], [18]–[20] conducted the transient analysis for load identification. Due to most of different electrical appliances having their unique electrical characteristic(s), they have partially or completely repeatable transient profiles [20]. In [18], the switching voltage transient eigenvectors for non-intrusive load monitoring are calculated by using continuous wavelet transform, which suffers heavy computational burden. And to effectively reduce the computation time, an energy spectrum of the wavelet transform coefficients in different scales calculated by the Perceval's Theorem is proposed in [8] and [19]. In addition, some researchers recognized the characteristic information can be fully extracted by taking the steady-state and transient-state features of the load into overall consideration [21], [22]. Hong *et al.* selected seven kinds of load features with combination of current; voltage, active power and reactive power, and implemented Fourier transform to achieve feature extraction [23]. Liang *et al.* used current waveform, active power,

reactive power, other steady-state features and open active transient-state waveform to decompose the load [24], [25]. He used dual-layer feature extraction framework to distinguish electric equipment through three aspects of steady state, transient state and user behavior [26].

Coupled with the above load signature methods, some researchers also undertake to introduce the pattern classification algorithm into the non-intrusive load identification. The pattern identification method firstly constructs the load signature including different equipment as its base model. The learning model (other than the predefined base) of the base is used to identify the mixed signal to achieve effective estimate of energy consumption of each equipment, which can be divided into two types, supervised learning and unsupervised learning. Recently, supervised learning-based algorithms propose to formulate new meta-features from aggregated power measurement sampled at 10-minute interval and utilize these features to train classical multi-label classifiers such as support vector machines [27], [28], k nearest neighbor [29], [30] and neural network [31], [32] and so on. It has been proven that the operation of high precision electrical appliances can be accurately identified, while this kind of approach is prone to over-training and over-fitting problems. Kolter *et al.* convert non-intrusive load monitoring recognition to single channel (smart meter is the only channel) blind separation problem [33]–[35]. The approach transforms the problem of maximizing the energy decomposition performance into a structural prediction problem, and provides a specific training for the energy decomposition task, and then puts forward the effective algorithm. Although it was a good example of a supervised learning-based approach, the shortcoming is that, it cannot be used for real-time disaggregation and the massive of sensors for appliance sub-metering need to be deployed. In contrast, load identification based on unsupervised learning can automatically detect the basic structure of data, which reduces manual intervention and enhances practicality. Generally the approach based on unsupervised learning makes use of differential Hidden Markov Models (HMM) and other variants of HMM in [36], [39], [40]. Reference [36] proposes to model the probability behavior of devices by using a variant of Hidden Markov Model. The disadvantage of this presented approach is that it only takes into account the appliances with only ON/OFF states. When the number of electrical equipment is superabundant, the recognition accuracy will declined and it is easy to fall into local optimum. To alleviate the aforesaid problem, Kolter and T Jakakola proposed an extended version of the hidden Markov model (i.e. Additive Factorial Hidden Markov model, AFHMM), on the basis of which household electrical equipment was modeled [39]. Compared with the previous algorithms, the AFAMAP algorithm is not affected by the local minimum, and the decomposition accuracy is better. However, due to its huge matrix of variables, computational cost is clearly too high for real-time applications. Reference [40] assumes that at most one appliance changes state within a short period and models the single appliance by adding duration modeling and

differential observations to the conventional HMM. However, how to solve NILM problems with this model has not been reported.

The load signature method can be used to detect and identify the variations owing to the status changes of load switch. However, equipment switch information is so fleeting that it is difficult to separate mixed load. Secondly, the threshold value of changes in load signature is too large to lead to accurate event detection results and readily ends with an increase in computational complexity. Currently, there are inadequate effective features that can exclusively identify different load status. By comparison, the pattern recognition algorithm is highly intelligent and flexible in identification criteria. Nevertheless due to the high complexity of this kind of algorithms, the complicated process and the difficulty in hardware implementation and the identification accuracy is greatly influenced by changes of load amount. In addition, the methods mentioned above are used to decompose the load status according to signal features. Due to the complicated steps of feature extraction and the difficulty to obtain complete data of independent load, there is less research in respect of signal separation. Consequently the full and complete method to decompose separate loads is a vacancy in this realm.

On the whole, the existing non-intrusive power load monitoring algorithms mainly construct the power load model based on the extracted electrical features along with using optimization techniques or pattern recognition technology to achieve identification of power load. However, all of these approaches have their respective deficiencies and are not very satisfied. Trying to improve this kind of algorithms and based on the signal model of non-intrusive load monitoring, one of the contributions of this paper is through using the sparseness of current frequency domain signal to obtain an optimal solution. By using this property, we can transform the underdetermined problem into an optimization problem, which can employ a two-step iterative shrinkage threshold algorithm to completely separate independent load waveform from mixed signals. Furthermore, this approach can simplify load identification process while ensuring the identification accuracy. Another contribution of this paper is to identify the load of decomposed complete waveform through the characteristic filter only by constructing the current characteristic filter group but without extracting load features. The identification process is simple and accurate, and the computational complexity is lower than that of feature extraction approach. Meanwhile, the hardware implementation problem of pattern recognition algorithms in practical application is solved to some degree.

This paper consists of the following sections: Section II introduces fundamentals of NILM and algorithm ideas. Section III presents complete process of the algorithm herein. Section IV demonstrates validation and analysis of actually measured load data. Finally a summary and some conclusions are provided in Section V.

II. FUNDAMENTALS AND ALGORITHM MODELS

A. FUNDAMENTALS OF NILM

NILM is designed to acquire the overall power consumption information of user loads at residential power entrances. Fig. 1 shows the NILM structure, which identifies the operation of individual loads through analysis and processing of overall power consumption information, thus allowing for real-time tracing and management of residential energy efficiency [41]. In contrast with traditional load monitoring technologies, it is unnecessary to install a test device for each load, so the acquiring and monitoring mechanism is quite simple for users. It is suitable for individual installation and more acceptable. NILM simplifies the acquiring and measuring mechanism, but the power consumption data of all loads is included in one signal collected [42]. Therefore, for NILM, it is critical to analyze and extract the information of individual loads from single signal acquired, and effectively achieve load identification.

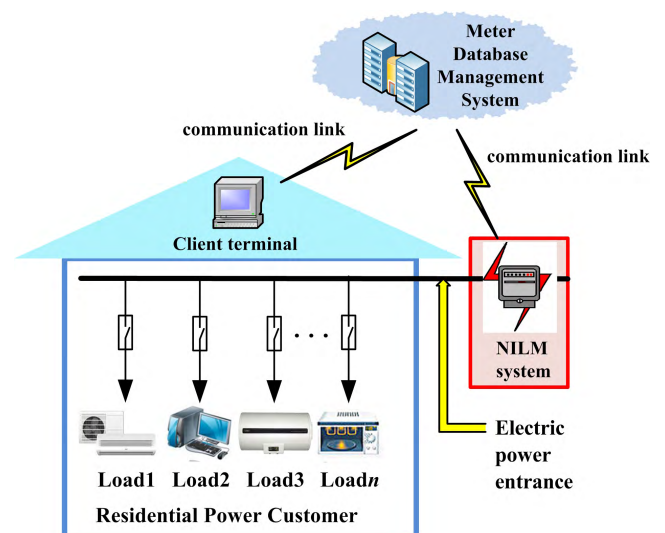


FIGURE 1. NILM structure.

B. LOAD DECOMPOSITION MODELS

The power consumption data of all loads is included in one comprehensive signal collected, out of which the power consumption information of individual loads should be separated and extracted. This paper is built upon the current signals of loads for decomposition and identification. In the event of m power consumption loads, the single current acquired in non-intrusive mode is as follows:

$$I(t) = \sum_{k=1}^m I_k(t) + n(t) \quad (1)$$

where $I_k(t)$ stands for the current signal of load operating independently, and $n(t)$ represents the signal of noise.

From (1) we can know that $I(t)$ is a known quantity, while $I_k(t)$ are unknowns to be solved, and there are m quantities in aggregate. Load decomposition can be modeled as solving

the underdetermined equation. However, when the number of loads, i.e., m , is far more than 1, the number of unknowns will be far more than equations, so the number of underdetermined dimensions will be huge. In this case, it will be difficult to solve the equation. Therefore, this paper will optimize the underdetermined issue.

According to the user habits in terms of load operation, there is very low probability to open or close two loads at the same time absolutely. That is, load switching is sequential. Therefore, the current operation model at present can be established as sum of current signal for the previous moment and individual load current newly put into operation, as shown in (2) below:

$$I(t) = \sum_{k=1}^{m-1} I_k(t) + I_m(t) + n(t) = I'(t) + I_m(t) + n(t) \quad (2)$$

where $I'(t)$ stands for the current signal at previous moment, and $I_m(t)$ stands for the independent current of load newly put into operation. Similarly, when there is a load off, the mixed current in the circuit is given by:

$$\begin{aligned} I(t) &= \sum_{k=1}^{m-1} I_k(t) + (-I_m(t)) + n(t) \\ &= I'(t) + (-I_m(t)) + n(t). \end{aligned} \quad (3)$$

Equation (2) or (3) indicates that, by solving two unknowns for each time interval, namely, mixed signal at previous moment and current signal of load newly put into operation, the multi-dimensional underdetermined issue of (1) can be transformed into one-dimensional underdetermined issue of (2) or (3), thus we can make sure that the equation can be solved effectively.

C. SOLUTION OF THE UNDERDETERMINED ISSUE

Solving only two unknown quantities at each time interval, the multi-dimensional underdetermined problem in (1) which is difficult to solve is transformed into the one-dimensional underdetermined problem in (2) or (3) which can be solved. To solve the underdetermined problem, (2) or (3) based on principle of compressed sensing is solved, and the sparseness of signal is used to construct the constraint conditions, thus to optimize the solution through iterative shrinkage.

Underdetermined problem can be deemed as high-dimensional unknown quantity to be projected to low-dimensional space through measurement matrix, as shown in (4)

$$\mathbf{I} = \Phi \Xi = \Phi \Psi \theta = \Theta \theta \quad (4)$$

where, Φ refers to the measurement matrix and \mathbf{I} refers to the vector representation of $I(t)$; Ξ refers to the decomposition current to be solved; Ψ refers to the sparse base of current signal; θ refers to the sparse representation of current. We cannot directly solve Ξ containing two unknown quantities from a measured value of \mathbf{I} . Therefore, based on the sparseness

of signal, we can achieve the sparsest solution [42] of the equation. The optimization problem is shown as (5)

$$\min \|\hat{\theta}\|_0 \quad \text{s.t. } \mathbf{I} = \Theta \hat{\theta} \quad (5)$$

where $\|\cdot\|_0$ refers to the norm of ℓ_0 , the number of nonzero elements in vector quantity. However, the solution of (5) can only be solved by solving all possible sparse situations and finding the sparsest form, which is a NP problem [43]. When multi-dimensional underdetermined problem is transformed into one-dimensional problem, ℓ_0 problem can be solved by equivalent to ℓ_1 norm problem, which is shown as (6). It can be equivalent to a linear programming problem, which is facilitated to use the existing method for solution

$$\min \|\hat{\theta}\|_1 \quad \text{s.t. } \mathbf{I} = \Theta \hat{\theta}. \quad (6)$$

To sum up, if there is a sparse base to make current signal sparse, the underdetermined problem in this paper can be solved. According to the periodicity of load current, the frequency domain component has harmonic property, in other words, only some specific frequency points have values, the remaining components are zeros, so the current signal in frequency domain has sparsity, and the sparse base is FFT transformation matrix [44].

D. ANALYSIS OF FREQUENCY DOMAIN CHARACTERISTICS OF RESIDENTIAL POWER LOADS

Current signals generated by the typical residential loads are acquired, and then are transformed into frequency domain. Fig. 2 shows the current spectrums of five different loads, with frequency f converted into digital angular frequency $\omega \in (-\pi, \pi)$ rad/s.

Fig. 2 indicates the harmonic property of current signal. The frequency domain characteristics of periodical signals lead to sparsity, which is the critical foundation to solve the underdetermined issues herein. The frequency components of load current are in the range of $-0.3\pi \sim 0.3\pi$ rad, which correspond to the frequency range of $0 \sim 1.5$ kHz. The characteristic frequency spectrums of all loads have power frequency of 50Hz ($\omega = 0.1\pi$) as fundamental; that is, all loads contain the frequency component, which has the highest energy.

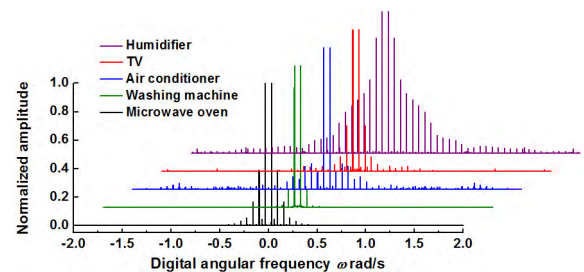


FIGURE 2. Current signal spectrums of different loads.

The frequency components of different power loads' current signals vary a great deal, in other words, the various loads have their specific spectrum components. The hardware

Circuits of different loads vary a great deal, and the oscillation frequencies and control signals of the circuits will introduce specific spectrum components, thus changing the original frequency intervals of signals. They are the critical foundation to use characteristic filtering for load identification. Furthermore, it shows more and more smart and digital electrical appliances, whose electronic circuits will introduce more high-frequency components, which represent low energy but are all characteristic components, providing favorable conditions for load identification.

III. LOAD IDENTIFICATION ALGORITHM BASED ON UNDERDETERMINED DECOMPOSITION AND CHARACTERISTIC FILTERING

In this paper, load decomposition is achieved by solving underdetermined problem, and the decomposition current signals of independent loads are obtained. Based on this, characteristic filtering is used for load identification. The processing details of the proposed algorithm are presented in this section.

A. DECOMPOSITION OF MIXED CURRENT SIGNALS

For residential users, the power consumption appliances are started and closed sequentially. In this section, the equation shown in (2) or (3) is solved, and two signals are separated for each time interval. One is the load current signal newly put into operation, and the other is the integrated current signal for previous moment. Equation (2) is expressed as (7):

$$\mathbf{I} = \mathbf{A}\mathbf{\Xi} + \mathbf{N} \quad (7)$$

where \mathbf{I} is the observed vector of collected single mixed current $I(t)$; $\mathbf{\Xi} = [\mathbf{I}', \mathbf{I}^m]^T$ is the unknown matrix consisting of two decomposed currents, and the length of \mathbf{I}' and \mathbf{I}^m is n ; $\mathbf{A} \in R^{n \times N}$ is the coefficient matrix, whose value is $[\mathbf{E}_{n \times n}, \mathbf{E}_{n \times n}]^T$ in ideal situation; and \mathbf{N} is the vector consisting of noises, which should be restricted in solving process. Similarly, when one load is off, the amplitude of the total load current will decrease, and from (3), the value of mixing matrix \mathbf{A} in our solution will be $[-\mathbf{E}_{n \times n}, \mathbf{E}_{n \times n}]^T$. As for the load decomposition process, i.e., solving $\mathbf{\Xi}$ with \mathbf{I} , since the number of unknowns is over the number of equations, it is necessary to set up the optimal objective function for solving.

In the optimization issue, the objective function is defined as follows:

$$f(\mathbf{\Xi}^k) = \underbrace{\frac{1}{2} \|\mathbf{I} - \mathbf{A}\mathbf{\Xi}^k\|_2^2}_I + \underbrace{\tau \Phi(\mathbf{\Xi}^k)}_{II} \quad (8)$$

where part I represents the fit goodness of known data, and part II is the regularization term, into which the expected characteristics of unknown signals are added to get the solution. And τ is the regular parameter. By adjusting its size, we can change the frequency domain sparsity of the separated signal. In each separation process, using the mixed matrix \mathbf{A} with the value of $[\mathbf{E}_{n \times n}, \mathbf{E}_{n \times n}]^T$ or $[-\mathbf{E}_{n \times n}, \mathbf{E}_{n \times n}]^T$, a mathematical model is constructed to indicate that the mixing current at the

previous moment is superimposed with the load current of the new input operation, and then by judging the frequency of the last mixed signal sparsity, adjust the regular coefficient τ to change the sparseness of the separation results to get the results we want. The estimated value sequence of unknown signal is $\{\mathbf{\Xi}^k, k = 0, 1, \dots, n\}$, where k stands for iteration number of the algorithm. The formula of iteration for solution is (9)

$$\mathbf{\Xi}^{k+1} = \arg \min_{\mathbf{\Xi}} \frac{1}{2} \|\mathbf{\Xi}^k - \mathbf{E}^k\|_2^2 + \frac{\tau}{\lambda} \Phi(\mathbf{\Xi}^k) \quad (9)$$

where $\mathbf{E}^k = \mathbf{\Xi}^k + \mathbf{A}^T(\mathbf{I} - \mathbf{A}\mathbf{\Xi}^k)/\lambda$, λ and τ are adjustable regularization parameters.

The regularization term in the equation adopts ℓ_1 norm of current signal to be solved; that is, $\Phi(\mathbf{\Xi}^k) = \|\mathbf{\Xi}^k\|_1$ is substituted into (9), which is shown as (10)

$$\mathbf{\Xi}^{k+1} = \arg \min_{\mathbf{\Xi}} \frac{1}{2} \|\mathbf{\Xi}^k - \mathbf{E}^k\|_2^2 + \frac{\tau}{\lambda} \|\mathbf{\Xi}^k\|_1. \quad (10)$$

With (10), we can take a derivative with respect to unknown $\mathbf{\Xi}$ as follows:

$$\mathbf{\Xi}^{k+1} = \arg \min_{\mathbf{\Xi}} \frac{1}{2} \|\mathbf{\Xi}^k - \mathbf{E}^k\|_2^2 + \frac{\tau}{\lambda} = \Gamma_{\lambda}(\mathbf{\Xi}^k) \quad (11)$$

where $\Gamma_{\lambda}(\mathbf{\Xi}^k)$ is a soft threshold function defined to remove the noise signals, and can be simplified as (12)

$$\Gamma_{\lambda}(\mathbf{\Xi}^k) = \text{sign}(\mathbf{\Xi}^k) \max\{|\mathbf{\Xi}^k| - \frac{\tau}{\lambda}, 0\}. \quad (12)$$

To sum up, the underdetermined problem in this paper can be simplified as (13).

$$f(\mathbf{\Xi}^k) = \frac{1}{2} \|\mathbf{I} - \mathbf{A}\mathbf{\Xi}^k\|_2^2 + \tau \|\mathbf{\Xi}^k\|_1. \quad (13)$$

The optimization issue shown in (13) can be solved through two-step iterations [45], and the process of iteration is shown as follows.

$$\begin{cases} \mathbf{\Xi}^1 = \Gamma_{\lambda}(\mathbf{\Xi}^0) \\ \mathbf{\Xi}^{k+1} = (1 - \alpha)\mathbf{\Xi}^{k-1} + (\alpha - \beta)\mathbf{\Xi}^k + \beta\Gamma_{\lambda}(\mathbf{\Xi}^k) \end{cases} \quad (14)$$

where $\mathbf{\Xi}^0$ is the initial value; α and β are adjustable parameters, with $0 < \alpha < 2$ and $0 < \beta < 2\alpha$. When $f(\mathbf{\Xi}^{k+1}) > f(\mathbf{\Xi}^k)$, the current value solved should be kept; when $f(\mathbf{\Xi}^{k+1}) < f(\mathbf{\Xi}^k)$, the iteration formula should be used to calculate $\mathbf{\Xi}^{k+2}$ with $\mathbf{\Xi}^k$ and $\mathbf{\Xi}^{k+1}$, and then whether the iteration is over can be determined by verifying if termination function is less than threshold value. The termination function is defined as (15)

$$C(\mathbf{\Xi}^{k+1}, \mathbf{\Xi}^k) = \frac{|f(\mathbf{\Xi}^{k+1}) - f(\mathbf{\Xi}^k)|}{f(\mathbf{\Xi}^k)}. \quad (15)$$

When the value of (15) is less than the termination threshold value, the iteration should be terminated, and the optimal solution of decomposed signal is obtained. Thus, the load current decomposition is finished. For each time interval, the iteration process is carried out. By this way we can make sure that the current of a load is effectively separated from the original mixed current when it is put into operation.

B. FREQUENCY DOMAIN FILTERING FOR LOAD IDENTIFICATION

After load decomposition, the current of the load which put into operation can be obtained independently, thus the complexity of load identification is greatly reduced. This paper puts forward an identification method based on frequency filtering.

$I_k(t)$ can be obtained a priori, which is called characteristic current of a load. The characteristic current of each load is regarded as a filter, which allows its own frequency components to pass only, while other frequency components will be filtered out. The frequency response of the characteristic current can be expressed as (16)

$$I_k(j\omega) = \begin{cases} |I_k(j\omega)| e^{j\varphi(\omega)} & \omega \in \omega_k \\ 0 & \omega \notin \omega_k \end{cases} \quad (16)$$

where ω_k is the frequency component of characteristic current signal $I_k(j\omega)$.

It is assumed that there are M power loads in a power consumption network. The characteristic currents of these loads constitute a group of frequency domain filters, which includes M branches. This group of filters is used to filter the decomposed load current signal $I_m(t)$ in frequency domain, and the result of filtering by each branch j is shown as (17)

$$Y_j(j\omega) = I_m(j\omega)I_j(j\omega) \approx \begin{cases} |I_m(j\omega)| |I_j(j\omega)| e^{j\theta(\omega)} & \omega \in \omega_j \cap \omega_m \\ 0 & \text{others} \end{cases} \quad (17)$$

where $I_m(j\omega)$ is the spectrum of decomposed current $I_m(t)$, ω_j and ω_m are the frequency components of $I_j(j\omega)$ and $I_m(j\omega)$. Equation (17) shows that, only when the frequency domain components of $I_j(j\omega)$ and $I_m(j\omega)$ are identical, can their spectral components be kept completely; otherwise, some frequency components will surely be restricted. Therefore, whether $I_m(t)$ is the load corresponding to the filter of the branch can be determined by verifying if the frequency component filtered is completely kept. After frequency domain filtering, if the frequency component of filtered output is apparently lost compared to $I_j(j\omega)$ or $I_m(j\omega)$, then $I_m(t)$ cannot be the load corresponding to $I_j(t)$. By contrast, if the frequency component of filtered output is completely kept, then $I_j(t)$ can be identified as the corresponding load.

In order to facilitate machine processing, the frequency components of filtering output are defined as 0-1. A threshold is selected as δ , when the frequency component above the threshold is set to 1, otherwise, it is set to 0. The binaryzation output can be expressed as (18)

$$y_j(j\omega) = \begin{cases} 1 & |Y_j(j\omega)| \geq \delta \\ 0 & |Y_j(j\omega)| < \delta. \end{cases} \quad (18)$$

Based on (18), the frequency components of $I_j(j\omega)$ and $I_m(j\omega)$ are quantified and recorded as $\hat{I}_j(j\omega)$ and $\hat{I}_m(j\omega)$, thus

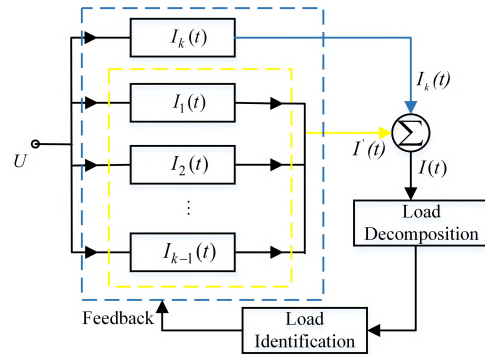


FIGURE 3. The concept schematic diagram.

the criterion function is established as (19) below:

$$\Gamma_1 = \frac{\sum_{\omega} y_j(j\omega)}{\sum_{\omega} \hat{I}_j(j\omega)} \quad \Gamma_2 = \frac{\sum_{\omega} y_j(j\omega)}{\sum_{\omega} \hat{I}_m(j\omega)}. \quad (19)$$

Equation (19) gives the quantitative criterion function of frequency component retention. When frequency component is completely kept after filtering, the ideal value of (19) is 1. Therefore, only when the values of Γ_1 and Γ_2 both are close to 1, can $I_m(t)$ be taken as the load corresponding to filter $I_j(j\omega)$.

C. PERFORMANCE ANALYSIS

The algorithm includes two parts. One part is load decomposition. Utilizing the load operation habits of residential users, it develops an optimization model for the underdetermined problems that are difficult to solve, then transforming them into one-dimensional underdetermined problem. In each processing interval, the processor collects the mixed current signal, and then establishes the mathematical solution model, while changing the regular parameter τ . The two-step iterative shrink threshold algorithm is used to recover the two source signals from the observed signal, one of which is the previous mixed signal and the other is the newly added load signal. The other part is load identification after decomposing the mixed signal. The frequency domain filters are constructed by the load characteristic currents obtained previously, and the frequency components are quantized to realize load identification after frequency domain filtering. The concept schematic diagram of the algorithm is presented in Fig. 3 and the implementation flow is shown in Fig. 4.

The condition for underdetermined optimization is that the loads are started and closed sequentially. If a load can be decomposed independently, the load decomposition and identification must be finished before next load start or off. Therefore, high processing efficiency is required, and the duration for decomposition and identification should be less than the minimum interval between which the user starts two loads. The major computation of load decomposition is solving the underdetermined equation, which is optimized into one-dimensional underdetermined issue to reduce solving

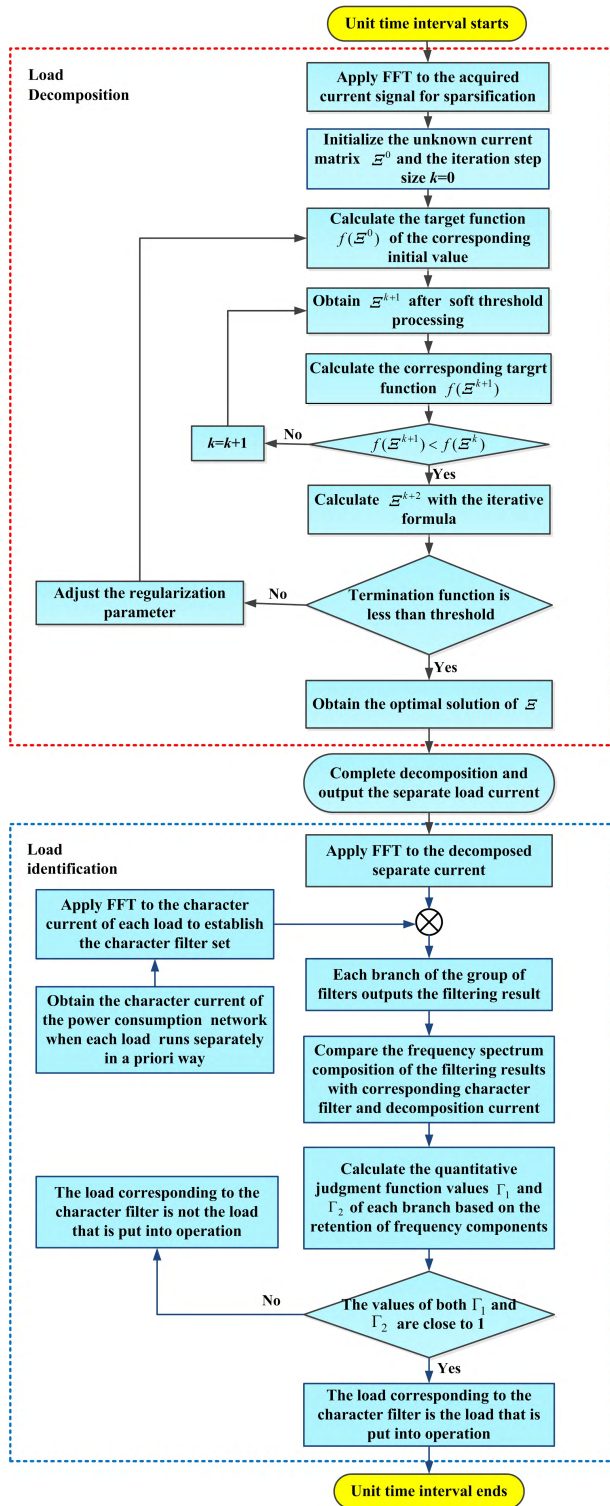


FIGURE 4. Flow chart of the proposed algorithm.

complexity. Two-step iteration threshold shrinkage is adopted in this process; that is, in the process of iteration, the information of previous iteration is used to improve computing speed and accelerate convergence process. The computing time of load decomposition can be controlled within 1.5s.

In the process of load identification, the current signals are transformed into frequency domain. This process can be realized by FFT and basic multiplication. Furthermore, final judgment of load identification is defined as 0-1 binaryzation form, which is suitable for machine processing. Therefore, it is easy to control the identification time within 0.5s via DSP. In combination, the implementation of the entire algorithm can be controlled within 2s, thus addressing the needs.

Decomposition models in this paper have conditions, using the time difference when the load started or closed. If two loads were started synchronously, mixed current of the two loads would be decomposed into one load, which could cause the error of load identification. In practice, the probability of being started absolutely synchronously two loads is small, so the condition has little influence. The reasons are as follows: Firstly, the habit of user’s operation determined that there are various lengths of time differences when the loads are started, even if the time difference is very small, but there often existed; Secondly, the response time is different when the loads are put in operation, therefore, even if the user operated two loads synchronously, there still are more obvious time differences on the signals. However, there still is the probability of being started synchronously. The algorithm could not completely eliminate the effects arising from being started synchronously, which could reduce the probability as much as possible. In this case, the direct optimization approach is to improve the convergence rate of the algorithm and reduce the unit interval for processing.

IV. EXPERIMENT AND ANALYSIS

In order to verify the effectiveness of the algorithm, a residential power consumption network is set up, and current signals of actual loads are acquired, with the signal sampling $f_s = 10\text{kHz}$. The algorithm is applied in load decomposition and identification.

Load decomposition is very important for the algorithm, so the method of solving underdetermined problem is verified firstly. Load switching process is that fan first starts when computer is running and then fridge starts. The loading process of experiment is shown in Fig. 5.

Fig. 6(a)-(c) show the current signal frequency domain waveforms of computer, fan and fridge respectively. There are values only at very few frequency components. As can be seen from the figure, their frequency spectrum values are zero (or the value is close to zero) at many frequency components, that is, there is less time when the frequency domain signal takes a larger value. In other words, the current signals are sparse in frequency domain.

Figure 7 shows the whole process of the algorithm. Fig. 7(a) indicates that the computer runs stably, and shows the spectrum of mixed current after the fan is connected. The proposed algorithm is used to decompose the mixed current, that is, by using the frequency domain sparsity of the load signal, the TWIST algorithm separates two signals from the mixed signal. In the process of algorithm separation, the value of regular coefficient needs to be set. After many

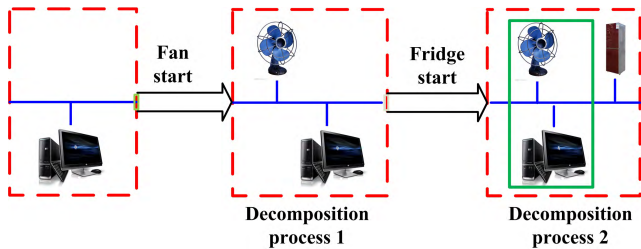


FIGURE 5. Load switching process.

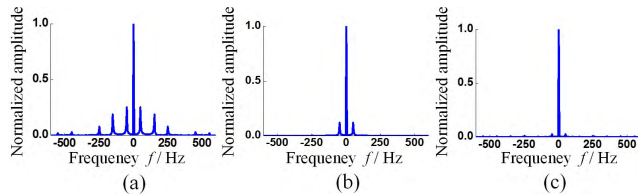


FIGURE 6. Load switching process. (a) computer. (b) Fan. (c) Fridge.

tests, the optimal coefficient $\tau = 3.0E - 9$ is obtained. Fig. 7(c)-(d) illustrate the two separated signals obtained after underdetermined solution, i.e., separated signal 1 and separated signal 2.

Compared with Fig. 6(a) and (b), although the two decomposition current signals are not completely consistent with the amplitude of the source signal, all the main frequency components are retained, which indicates that the separation is effective. In order to quantitatively evaluate the effectiveness of decomposition, the similarity coefficient is used to measure the degree of approximation between decomposed signals and original current signals as follows:

$$\rho = \frac{\left| \sum_{i=1}^M (x_i - \bar{x})(y_i - \bar{y}) \right|}{\sqrt{\sum_{i=1}^M (x_i - \bar{x})^2} \sqrt{\sum_{i=1}^M (y_i - \bar{y})^2}} \quad (20)$$

where x and y are the two sequences compared, and M is the number of sequence points. When ρ approaches to 1, the two sequences are more similar. Table 1 provides the values of similarity coefficient between separated signals and original current signals. The values approach to 1, indicating that the separated signals retain the original ones well. Major frequency components and scale are well kept. After each load is decomposed, the decomposition current is recognized by the characteristic frequency domain filter composed of the computer, the fan and the refrigerator. Each filter filters the decomposed current, and its decision results are displayed on the lower side of the decomposition current. Frequency components of filtering output must be not lost after comparing with the characteristic filter spectrum and decomposition current spectrum. In this case, it could decide that the corresponding load is put into operation of the frequency domain filter.

TABLE 1. Coefficient of similarity between separated signals and original current signals in frequency domain.

Load	Computer	Fan	Fridge	Mixed signal
Coefficient	0.9511	0.9817	0.9031	0.8997

Fig. 7 shows that for the separated signal 1, only after passed the frequency domain filter of fan, compared with the corresponding decomposition current and frequency domain filter, the output frequency components are completely retained. But after passed the corresponding frequency domain filter of other two kinds of loads, compared with at least one kind, the output frequency components appeared obvious losses. Only the second output in Fig. 7, relative to the former two, was completely retained, so that the load could be identified as fan. The identification process of the separation signal 2 is similar.

Fig. 7(b), (e)-(f) present the process of decomposition after connection running of fridge. The mixed signal of computer and fan is then recorded as one original signal. When the fridge is started, there are still two signals need to be decomposed. One signal is the mixed current of computer and fan which have finished the decomposition at the previous processing interval, and the other is the current of fridge that is newly put into operation at this processing interval. Fig. 7(b) demonstrates the spectrum of mixed current signal after the fridge is put into operation, The proposed algorithm is used to decompose the mixed current as shown in Fig. 7(e)-(f), and the decomposed signal with different sparsity can be obtained by modifying the value of the regular coefficient $\tau = 1.5E - 9$. The decomposition signal 3 is shown in Fig. 7(e), and the decomposition signal 4 is shown in Fig. 7(f). As can be seen from the comparison with Fig. 7(a) and Fig. 6(c), the decomposition signal 3 corresponds to the mixed signal of the computer and the fan, and the decomposition signal 4 corresponds to the refrigerator signal. It is clear that the two separated signals and the original signals basically share the same spectrum. As Fig. 7 revealed, all loads are decomposed independently, so the load decomposition method is effective. Similarly, after each load is decomposed, the decomposition current is recognized by the characteristic frequency domain filter composed of the computer, the fan and the refrigerator. The separation current 3 is corresponding to the cooperation of the computer and the fan. Therefore, after the characteristic filtering, the frequency components of the filtered output are lost varying degrees compared with the frequency domain filter spectrum and the decomposed current spectrum. So, through the decision recognition, the separation current 3 is not the open appliance. At the same time, as shown in the lower side of the decomposition current 3 of Fig. 7(f), the refrigerator signal has been correctly identified.

To demonstrate the verification, a small power consumption network is established. Five loads are selected consisting

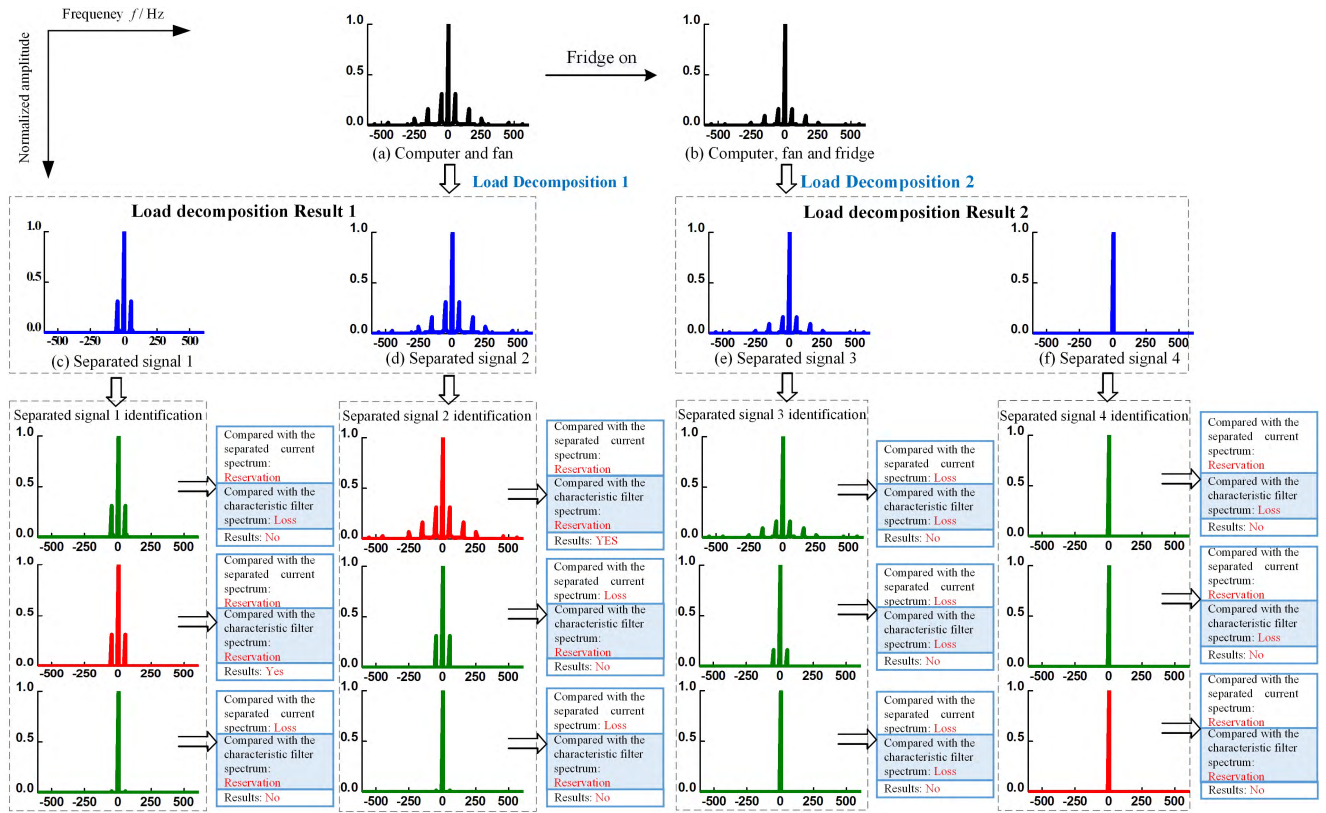


FIGURE 7. Results of load decomposition and identification.

TABLE 2. Coefficient of similarity between separated signals and original current signals in time domain.

Load	Load1	Load2	Load3	Load4	Load5
Coefficient	0.8511	0.9968	0.9987	0.89981	0.8206

of fan, fridge, rice cooker, air conditioner and TV set, which are typical residential loads and cover the various types of power loads, including resistance, motor and switching power supply. Two lines of current signals are separated in unit time interval, and all loads can be decomposed independently in different time intervals.

Fig. 8 shows the current signal waveforms of the five loads that run separately in time domain. Load1 to load5 are fan, fridge, rice cooker, air conditioner and TV set, successively. Fig. 9 shows the decomposed currents of the loads obtained by load decomposition. The left side of Fig. 9 (including Fig. 9(a), Fig. 9(b), Fig. 9(c), Fig. 9(d) and Fig. 9(e)) labeled in blue shows the current signals' spectrum of five power loads. The right side of Fig. 9 (including Fig. 9(f), Fig. 9(g), Fig. 9(h), Fig. 9(i) and Fig. 9(j)) labeled in green shows the decomposed current signal of the five loads in frequency domain. The spectrums of the source signals and the decomposed signals are sparse and the spectral components are substantially the same.

The decomposition process for each time interval is 1.5s on average, so the method is able to address our needs and allows for real-time decomposition. Comparing the decomposed current signals shown in Fig. 10 with the original load current signals shown in Fig. 8, it can be seen that the decomposed signals and original signals share very similar waveforms. Table 2 gives the time domain similarity coefficient of load current signals corresponding to the decomposed current signals. As Table 2 revealed the similarity coefficients of load 2 and load 3 are above 0.99, indicating very high similarity. The similarity coefficients for decomposed currents of load 1, load 4 and load 5 are relatively low, but this have no influence on the load identification.

The loads in the power network were put into operation in turn from the off state. During the experiment, the processing interval was 3s. Load decomposition must be conducted within each processing interval. If there were loads put into operation within the interval, the current of new load being put into operation could be decomposed out independently, and within the interval, the decomposed load being put into operation was conducted identification. Transforming the load current decomposed out to the frequency domain by FFT, and conducting the frequency domain filtering by priori building the characteristic filter group, each branch would have filtering output. In this case, the frequency components of the filtering output were compared with that of the load

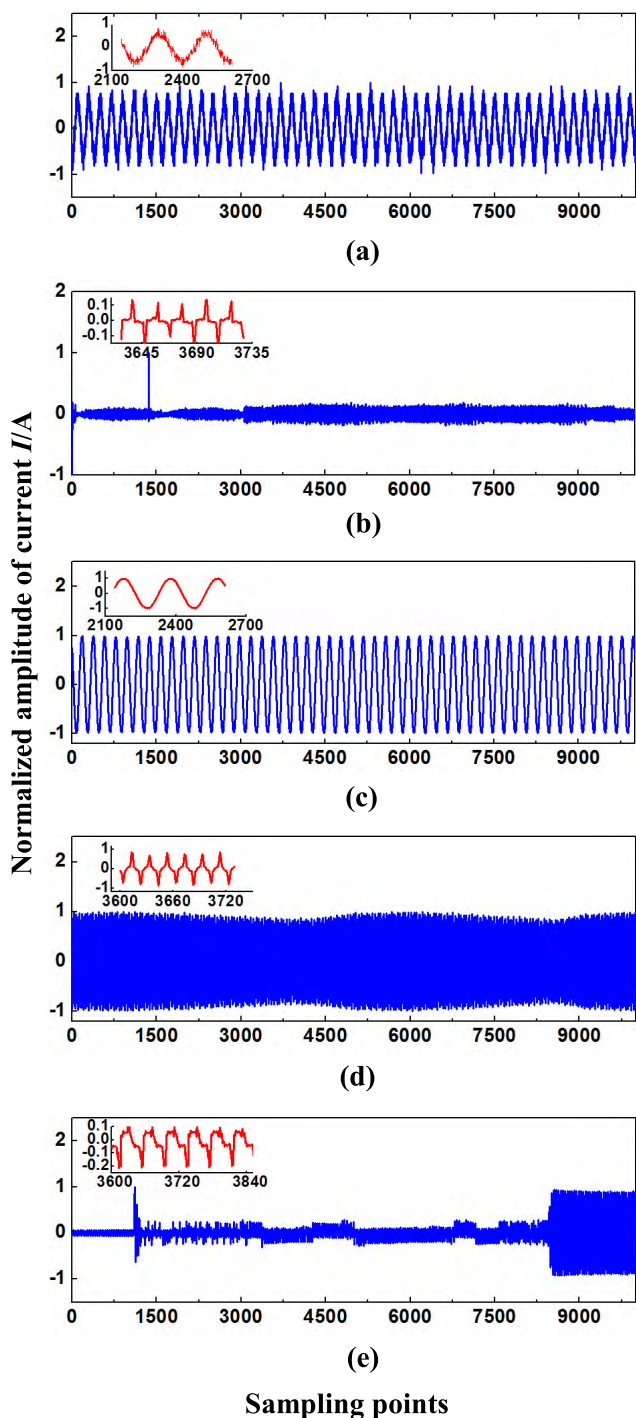


FIGURE 8. Current signals of five power loads. (a) load 1–fan. (b) load 2–fridge. (c) load 3–rice cooker. (d) load 4–air conditioner. (e) load 5–TV.

current spectrum and that of the corresponding frequency domain filter, respectively. If there were no obvious losses for the frequency component, the load being put into operation was the corresponding one in the frequency domain filter of this branch.

In order to facilitate the machine’s decision, the parameters were constructed in accordance with degree of preserving

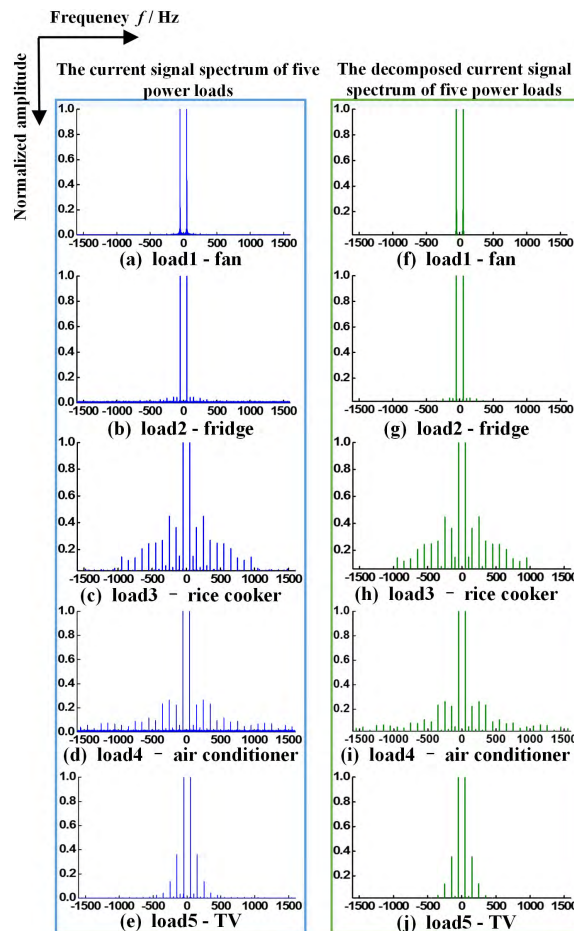


FIGURE 9. The current signals and decomposed current signals spectrum of five power loads.

TABLE 3. Quantitative decision results.

Decomposed currents	Characteristic filters					
	Load1	Load2	Load3	Load4	Load5	
Load1	Γ_1	0.9961	1.0000	0.3684	0.5203	0.6250
	Γ_2	1.0000	0.1321	0.1531	0.0943	0.0943
Load2	Γ_1	0.1509	0.9986	0.2632	0.4000	0.5003
	Γ_2	0.9973	1.0000	0.7143	0.5714	0.5285
Load3	Γ_1	0.2312	0.7143	0.9853	0.5107	0.7500
	Γ_2	0.3684	0.2632	0.9968	0.2632	0.3158
Load4	Γ_1	0.7594	0.5714	0.2632	0.9937	0.3750
	Γ_2	0.0943	0.4102	0.5000	1.0000	0.5371
Load5	Γ_1	0.1969	0.5714	0.3158	0.3241	0.9871
	Γ_2	0.6250	0.5215	0.7500	0.3750	0.9735

of the frequency component, namely (19). The decision was conducted according to the decision parameters of (19) in the experiment. Only two decision parameters both were close to 1, the running load was the corresponding one in the

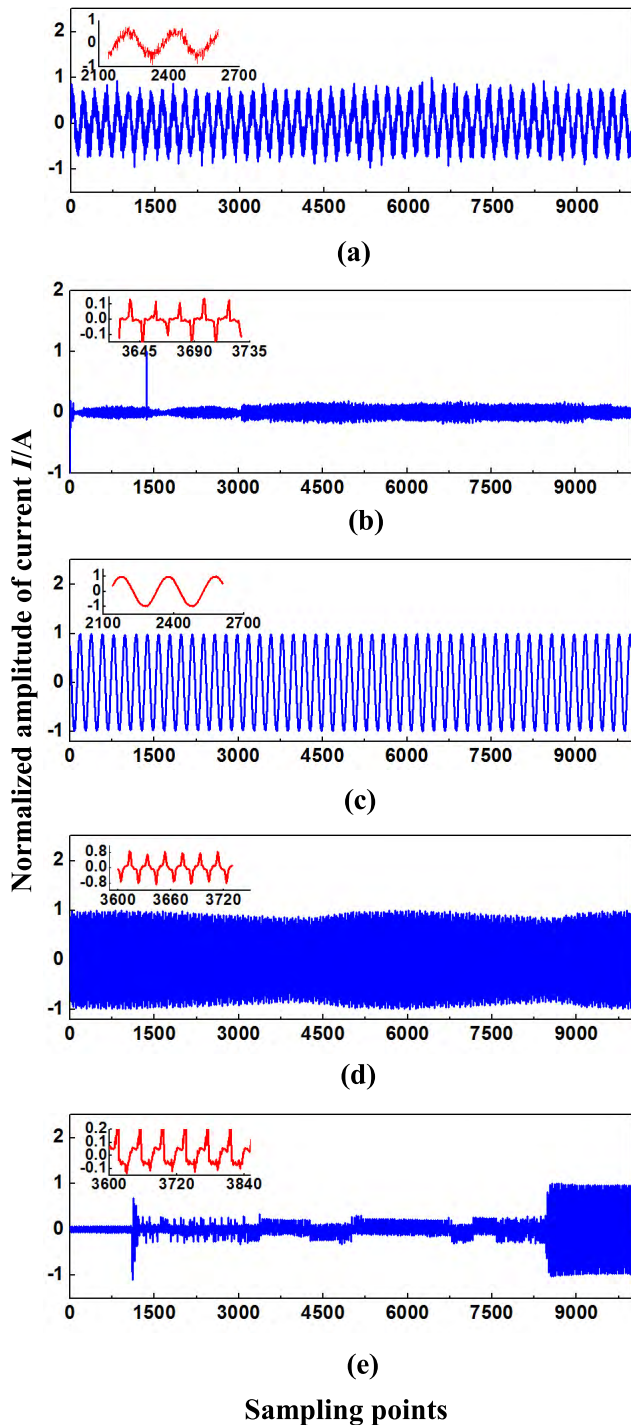


FIGURE 10. Decomposed current signals of the five power loads. (a) load 1—fan. (b) load 2—fridge. (c) load 3—rice cooker. (d) load 4—air conditioner. (e) load 5—TV.

frequency domain filter of this branch. As long as there was a parameter being less than 1, it was not the corresponding load. There were five times to put the load into operation in the experiment, thus the respective current was decomposed out in five intervals respectively, and load identification was conducted. The decision parameters were shown in Table 3.

Table 3 provides the quantitative identification parameters for all loads. Only with the frequency domain filtering corresponding to the load can the frequency component be well kept. As a result, both identification parameters approach 1, and dual parameters allow for the accuracy of identification. From Table 3, it is known that all loads can be accurately identified.

Since the identification process after decomposition is similar, we provide the result of identification after the fourth decomposition, i.e., the result of frequency domain filtering after the air conditioning is decomposed, as shown in Fig. 11. The subgraph labeled in green of Fig. 11 is the air conditioning current waveform in frequency domain after the fourth load decomposition. The left side of Fig. 11 labeled in blue is the corresponding frequency domain filter spectrum of each load. The middle labeled in red is the frequency component after each filter conducted the filtering for the air conditioning decomposition current, and the decision result is on the right.

Frequency components of filtering output must remain relatively complete after comparing with the frequency domain filter spectrum and decomposition current spectrum. In this case, it could be decided that the corresponding load that put into operation. Fig. 11 shows that for the current signals after independent decomposition, only after they passed the frequency domain filter of air conditioning (load 4), compared with the decomposition current and the frequency domain filter, the output frequency components were completely retained. But after they passed the frequency domain filters of other four loads, compared with at least one kind, the output frequency components appeared obvious losses. Only the fourth output in Fig. 11, relative to the former two, was completely retained, so that the load could be identified as air conditioning.

Fig. 12 compares the proposed algorithm, traditional time domain algorithm and Fisher intelligent algorithm with the increase in the number of loads in terms of computational efficiency and identification accuracy rate.

Traditional time domain identification algorithm uses the change of load signature to conduct judgment for load switching. Load signature refers to the unique information that can reflect the electrical state embodied in the operating electrical equipment, such as active power waveform [25]. After detecting the load of the switch, the effective value and the maximum value of load current and voltage are extracted further in time domain. Afterwards, the genetic algorithm is used to compare the given features of the electrical equipment and the load features extracted from the measured data to identify the components of the mixed load. Then the basic transform domain analysis of load identification is carried out. Traditional optimization algorithm achieves the goal of identifying load by studying the featured models of each load. Computational efficiency and identification accuracy of the traditional algorithm are greatly influenced by the load features, depending on the dimensions and effectiveness of the features. Fisher intelligent algorithm is a linear discriminant algorithm [46]. When non-intrusive monitoring is used to

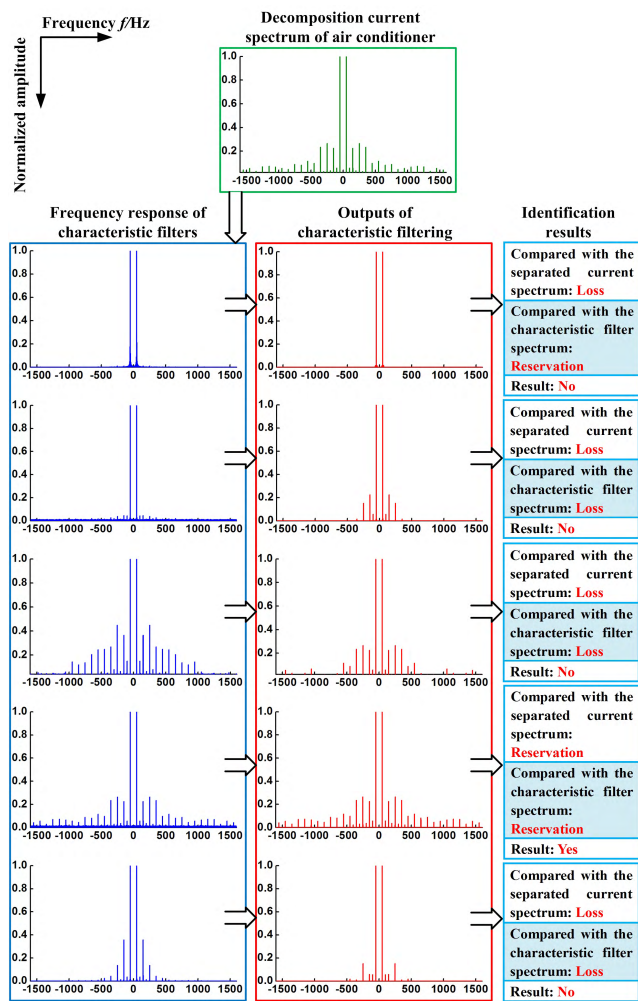


FIGURE 11. Identification process of air conditioning after it is decomposed independently.

extract the load feature, it uses the Fisher intelligent algorithm with supervisory discrimination to select the projection line and projects the data points of the main component feature space on a straight line to separate the load data, thus to achieve load identification.

Fig. 12(a) shows that the number of frequency domain filters increases with the increase in the number of loads. The calculated amount of this paper has a slight increase, but the increase of calculation complexity has little effect on the whole identification efficiency. Under the circumstance of lower feature dimension, the processing efficiency of the traditional time domain algorithm continuously fluctuates around 2.2s, but its processing efficiency is related to the time domain feature. As the feature increases, the computational efficiency will sharply fall. Fisher intelligent algorithm needs to extract the load features and conduct linear iteration, so the calculated amount is large and the computing time is longer. Fig. 12(b) shows that the identification accuracy curves of the three algorithms as the number of input loads increase. As the number of loads changes, the accuracy of the proposed

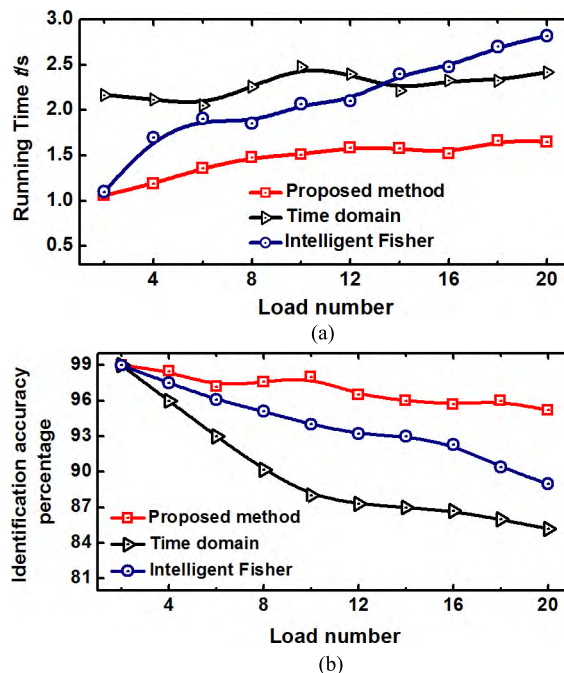


FIGURE 12. Performance comparison. (a) Computational efficiency. (b) Identification accuracy.

algorithm is less affected. However, the traditional approach is more sensitive to the increase of load number, which caused a significant decrease of the identification accuracy. Similarly, fisher algorithm also has a significant decrease in identification accuracy rate as the feature increases.

V. CONCLUSION

A non-intrusive identification algorithm for residential users based on underdetermined decomposition and frequency domain filtering is proposed.

The undetermined solution model of current is established for load decomposition. The sparse feature of current in frequency domain is used to transform the underdetermined problem into optimization seeking problem. Two-step iterative shrinkage threshold algorithm is introduced to enable the solving process to rapidly converge. As the experimental results demonstrated, this algorithm can competently separate the waveform of each load from the mixed currents. The decomposed current is filtered in frequency domain. We can judge the retention of the output frequency component to complete load identification. The judgment function in two-parameter form is constructed to ensure the accuracy of load identification. The performance is validated by the actually measured data. The computational efficiency and identification accuracy have been improved obviously compared with traditional method.

In this paper, the regularization parameters are determined by experience value. This has influence to the convergence rate and decomposition accuracy. Therefore, it is required to further study the adaptive parameter selection strategy, guiding the solution to the direction of optimal solution.

REFERENCES

- [1] D. He, W. Lin, N. Liu, R. G. Harley, and T. G. Habetler, "Incorporating non-intrusive load monitoring into building level demand response," *IEEE Trans. Smart Grid*, vol. 4, no. 4, pp. 1870–1877, Dec. 2013.
- [2] P. Siano, "Demand response and smart grids—A survey," *Renew. Sustain. Energy Rev.*, vol. 30, pp. 461–478, Feb. 2014.
- [3] F. Iglesias, P. Palensky, S. Cantos, and F. Kupzog, "Demand side management for stand-alone hybrid power systems based on load identification," *Energies*, vol. 5, no. 11, pp. 4517–4532, 2012.
- [4] S. Tian, B. Wang, and J. Zhang, "Key technologies for demand response in smart grid," *Proc. CSEE*, vol. 34, no. 22, pp. 3576–3589, 2014.
- [5] S. Wang, Z. Sun, and Z. Liu, "Co-scheduling strategy of home energy for smart power utilization," *Autom. Electr. Power Syst.*, vol. 39, no. 17, pp. 108–113, 2015.
- [6] Y. Y. Zhang et al., "Optimal energy management of a residential local energy network based on model predictive control," *Proc. CSEE*, vol. 35, no. 14, pp. 3656–3666, 2015.
- [7] S. Tomproš, N. Mouratidis, M. Draaijer, A. Foglar, and H. Hrasnica, "Enabling applicability of energy saving applications on the appliances of the home environment," *IEEE Netw.*, vol. 23, no. 6, pp. 8–16, Nov./Dec. 2009.
- [8] H. H. Chang, K. L. Chen, Y. P. Tsai, and W. J. Lee, "A new measurement method for power signatures of nonintrusive demand monitoring and load identification," *IEEE Trans. Ind. Appl.*, vol. 48, no. 2, pp. 764–771, Mar./Apr. 2012.
- [9] P. Li and Y. Yu, "Non-intrusive method for on-line power load decomposition," *J. Tianjin Univ.*, vol. 42, no. 2, pp. 1–8, 2009.
- [10] G. W. Hart, "Nonintrusive appliance load monitoring," *Proc. IEEE*, vol. 80, no. 12, pp. 1870–1891, Dec. 1992.
- [11] H. G. C. P. Dinesh, D. B. W. Nettasinghe, G. M. R. I. Godaliyadda, M. P. B. Ekanayake, J. V. Wijayakulasooriya, and J. B. Ekanayake, "A subspace signature based approach for residential appliances identification using less informative and low resolution smart meter data," in *Proc. 9th Int. Conf. Ind. Inf. Syst.*, Dec. 2014, pp. 1–6.
- [12] H. G. C. P. Dinesh, P. H. Perera, G. M. R. I. Godaliyadda, M. P. B. Ekanayake, and J. B. Ekanayake, "Individual power profile estimation of residential appliances using low frequency smart meter data," in *Proc. IEEE 10th Int. Conf. Ind. Inf. Syst.*, Dec. 2015, pp. 140–145.
- [13] M. Dong, P. C. M. Meira, W. Xu, and W. Freitas, "An event window based load monitoring technique for smart meters," *IEEE Trans. Smart Grid*, vol. 3, no. 2, pp. 787–796, Jun. 2012.
- [14] Y. Xu and J. V. Milanović, "Artificial-intelligence-based methodology for load disaggregation at bulk supply point," *IEEE Trans. Power Syst.*, vol. 30, no. 2, pp. 795–803, Mar. 2015.
- [15] H. Y. Lam, G. S. K. Fung, and W. K. Lee, "A novel method to construct taxonomy electrical appliances based on load signature," *IEEE Trans. Consum. Electron.*, vol. 53, no. 2, pp. 653–660, May 2007.
- [16] T. Hassan, F. Javed, and N. Arshad, "An empirical investigation of V-I trajectory based load signatures for non-intrusive load monitoring," *IEEE Trans. Smart Grid*, vol. 5, no. 2, pp. 870–878, Mar. 2014.
- [17] N. Henaou, K. Agbossou, S. Kelouwani, Y. Dubé, and M. Fournier, "Approach in nonintrusive type I load monitoring using subtractive clustering," *IEEE Trans. Smart Grid*, vol. 8, no. 2, pp. 812–821, Mar. 2017.
- [18] C. Duarte, P. Delmar, K. W. Goossen, K. Barner, and E. Gomez-Luna, "Non-intrusive load monitoring based on switching voltage transients and wavelet transforms," in *Proc. IEEE Future Instrum. Workshop*, Gatlinburg, TN, USA, Oct. 2012, pp. 1–4.
- [19] H.-H. Chang, K.-L. Lian, Y.-C. Su, and W.-J. Lee, "Power-spectrum-based wavelet transform for nonintrusive demand monitoring and load identification," *IEEE Trans. Ind. Appl.*, vol. 50, no. 3, pp. 2081–2089, May/June 2014.
- [20] Y.-H. Lin and M.-S. Tsai, "Development of an improved time–frequency analysis-based nonintrusive load monitor for load demand identification," *IEEE Trans. Instrum. Meas.*, vol. 63, no. 6, pp. 1470–1483, Jun. 2014.
- [21] S. B. Leeb, S. R. Shaw, and J. L. Kirtley, Jr., "Transient event detection in spectral envelope estimates for nonintrusive load monitoring," *IEEE Trans. Power Del.*, vol. 10, no. 3, pp. 1200–1210, Jul. 1995.
- [22] S. M. Tabatabaei, S. Dick, and W. Xu, "Toward non-intrusive load monitoring via multi-label classification," *IEEE Trans. Smart Grid*, vol. 8, no. 1, pp. 26–40, Jan. 2017.
- [23] Y.-Y. Hong and J.-H. Chou, "Nonintrusive energy monitoring for microgrids using hybrid self-organizing feature-mapping networks," *Energies*, vol. 5, no. 7, pp. 2578–2593, 2012.
- [24] J. Liang, S. K. K. Ng, G. Kendall, and J. W. M. Cheng, "Load signature study—Part II: Disaggregation framework, simulation, and applications," *IEEE Trans. Power Del.*, vol. 25, no. 2, pp. 561–569, Apr. 2010.
- [25] H. Ahmadi and J. R. Martí, "Load decomposition at smart meters level using eigenloads approach," *IEEE Trans. Power Syst.*, vol. 30, no. 6, pp. 3425–3436, Nov. 2015.
- [26] D. He, L. Du, Y. Yang, R. Harley, and T. Habetler, "Front-end electronic circuit topology analysis for model-driven classification and monitoring of appliance loads in smart buildings," *IEEE Trans. Smart Grid*, vol. 3, no. 4, pp. 2286–2293, Dec. 2012.
- [27] Y.-X. Lai, C.-F. Lai, Y.-M. Huang, and H.-C. Chao, "Multi-appliance recognition system with hybrid SVM/GMM classifier in ubiquitous smart home," *Inf. Sci.*, vol. 230, pp. 39–55, May 2013.
- [28] M. Singh, S. Kumar, S. Semwal, and R. S. Prasad, "Residential load signature analysis for their segregation using wavelet—SVM," *Power Electron. Renew. Energy Syst.*, vol. 326, pp. 863–871, Nov. 2015.
- [29] M.-S. Tsai and Y.-H. Lin, "Modern development of an adaptive non-intrusive appliance load monitoring system in electricity energy conservation," *Appl. Energy*, vol. 96, pp. 55–73, Aug. 2012.
- [30] T. Saitoh, T. Osaki, R. Konishi, and K. Sugahara, "Current sensor based home appliance and state of appliance recognition," *J. Control, Meas., Syst. Integr.*, vol. 3, no. 2, pp. 86–93, 2010.
- [31] T. Bier, D. O. Abdeslam, J. Merckle, and D. Benyoucef, "Smart meter systems detection & classification using artificial neural networks," in *Proc. IEEE 38th Annu. Conf. Ind. Electron. Soc.*, Montreal, QC, Canada, Oct. 2012, pp. 3324–3329.
- [32] Y.-H. Lin and M.-S. Tsai, "A novel feature extraction method for the development of nonintrusive load monitoring system based on BP-ANN," in *Proc. Int. Symp. Comput. Commun. Control Autom.*, Tainan, Taiwan, May 2010, pp. 215–218.
- [33] J. Z. Kolter, S. Batra, and A. Y. Ng, "Energy disaggregation via discriminative sparse coding," in *Proc. Int. Conf. Neural Inf. Process. Syst.*, Vancouver, BC, Canada, 2010, pp. 1153–1161.
- [34] E. Elhamifar and S. Sastry, "Energy disaggregation via learning 'powerlets' and sparse coding," in *Proc. 29th AAAI Conf. Artif. Intell.*, Austin, TX, USA, 2015, pp. 629–635.
- [35] M.-P. Hosseini, H. Soltanian-Zadeh, K. Elisevich, and D. Pompili, "Cloud-based deep learning of big eeg data for epileptic seizure prediction," in *Proc. IEEE Global Conf. Signal Inf. Process.*, Dec. 2016, pp. 1151–1155.
- [36] H. Kim, M. Marwah, M. F. Arlitt, G. Lyon, and J. Han, "Unsupervised disaggregation of low frequency power measurements," in *Proc. 11th SIAM Int. Conf. Data Mining*, Mesa, AZ, USA, 2011, pp. 28–30.
- [37] J. Z. Kolter and T. Jaakkola, "Approximate inference in additive factorial HMMs with application to energy disaggregation," *J. Mach. Learn. Res.*, vol. 22, pp. 1472–1482, Mar. 2012.
- [38] S. Makonin, F. Popowich, I. V. Bajic, B. Gill, and L. Bartram, "Exploiting HMM sparsity to perform online real-time nonintrusive load monitoring," *IEEE Trans. Smart Grid*, vol. 7, no. 6, pp. 2575–2585, Nov. 2016.
- [39] J. Z. Kolter and T. Jaakkola, "Approximate inference in additive factorial HMMs with application to energy disaggregation," in *Proc. 15th Int. Conf. Artif. Intell. Stat.*, La Palma, Spain, 2012, pp. 1472–1482.
- [40] Z. Guo, Z. J. Wang, and A. Kashani, "Home appliance load modeling from aggregated smart meter data," *IEEE Trans. Power Syst.*, vol. 30, no. 1, pp. 254–262, Jan. 2015.
- [41] J. Liang, S. K. K. Ng, G. Kendall, and J. W. M. Cheng, "Load signature study—Part I: Basic concept, structure, and methodology," *IEEE Trans. Power Del.*, vol. 25, no. 2, pp. 551–560, Apr. 2010.
- [42] X.-X. Zheng, Q.-Q. Liu, S.-F. Lin, D.-D. Li, and M. Zhang, "Research of the microscopic signatures of residential loads for NILM," *Power Syst. Protection Control*, vol. 42, no. 10, pp. 62–70, 2014.
- [43] M. Elad, "Sparse and redundant representation modeling—What next?" *IEEE Signal Process. Lett.*, vol. 19, no. 12, pp. 922–928, Dec. 2012.
- [44] P. Cheng, *Digital Signal Processing*. Beijing, China, Tsinghua Press, 2012.
- [45] J. M. Bioucas-Dias and M. A. T. Figueiredo, "A new TwIST: Two-step iterative shrinkage/thresholding algorithms for image restoration," *IEEE Trans. Image Process.*, vol. 16, no. 12, pp. 2992–3004, Dec. 2007.
- [46] B. Qi, Y. Cheng, and X. Wu, "Non-intrusive household appliance load identification method based on fisher supervised discriminant," *Power Syst. Technol.*, vol. 40, no. 8, pp. 2484–2490, 2016.



and power system information processing technology.

XIN WU received the B.E. degree in electrical engineering from North China Electric Power University in 2007 and the Ph.D. degree in communication and information systems from the Institute of Electronics, Chinese Academy of Sciences, in 2012. She is currently a Faculty Member with the School of Electrical and Electronic Engineering, North China Electric Power University. Her research interests include smart grid applications, power system measurements,



LIYA LIU received the B.Eng. degree in communication engineering from North China Electric Power University in 2016, where she is currently pursuing the M.E. degree in information and communication engineering. Her research interests include intelligent power information processing and non-intrusive load monitoring.



XIAO HAN was born in Chifeng, Inner Mongolia Autonomous Region, China, in 1994. She received the B.S. degree in communications engineering from North China Electric Power University, Beijing, in 2016, where she is currently pursuing the M.S. degree in information and communication engineering. Her research interests include the smart electricity and power system information processing technology.



BING QI received the B.E. and M.A. degrees in electrical engineering from Beijing Jiaotong University. He is currently a Professor with North China Electric Power University. His research interests include demand side management of smart grid and electric power communication technology. He is a Technical Expert of IEC PC-118.

• • •